Loss of BAP1 Results in Growth Inhibition and Enhances Mesenchymal–Epithelial Transition in Kidney Tumor Cells

Authors

Pengsheng Chen, Huan Wang, Wenhao Zhang, Yuling Chen, Yang Lv, Di Wu, Mingzhou Guo, and Haiteng Deng

Correspondence

dht@tsinghua.edu.cn

In Brief

Lower expression of WT *BAP1* was correlated with longer overall survival in ccRCC patients. Quantitative proteomic analysis revealed that BAP1 was largely involved in cytoskeletal remodeling and cell proliferation. Functional assays determined that loss of *BAP1* decreased cell motility and inhibited cell proliferation in ccRCC cell lines. *BAP1* knockout rendered accumulation of H2AK119ub on the *Snail* gene region and inhibited *Snail* transcription, and thus led to mesenchymal-epithelial transition in ccRCC tumor cells.

Graphical Abstract

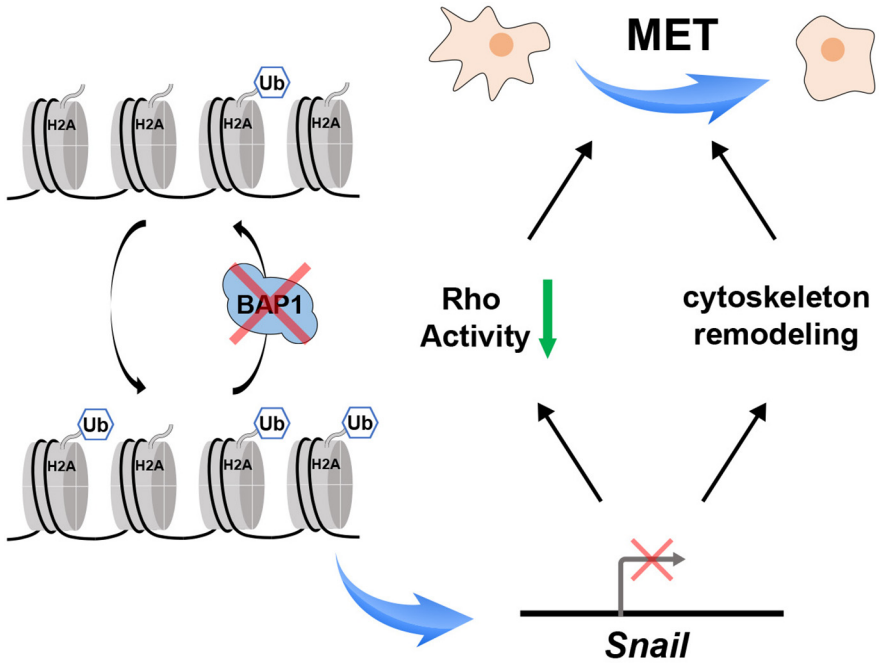

Highlights

- Proteomic analysis revealed that BAP1 was involved in cell motility and morphology.
- Loss of *BAP1* promoted MET and inhibited cell proliferation.
- Rho GTPase family participated in the MET induced by *BAP1* knockout.
- Loss of *BAP1* increased H2AK119ub on *Snail* gene and inhibited *Snail* transcription.

Chen et al., 2019, Molecular & Cellular Proteomics *18*, 1320–1329

https://doi.org/10.1074/mcp.RA119.001457

Loss of BAP1 Results in Growth Inhibition and Enhances Mesenchymal–Epithelial Transition in Kidney Tumor Cells*[S]

Pengsheng Chen‡, Huan Wang§, Wenhao Zhang‡, Yuling Chen‡¶, Yang Lv‖, Di Wu‖, Mingzhou Guo‖, and Haiteng Deng‡**

BRCA1-associated protein 1 (BAP1) is a member of the ubiquitin C-terminal hydrolase family of deubiquitinating enzymes and is implicated in transcriptional regulation. The *BAP1* gene is mutated in about 10% of patients with ccRCC, the most common form of renal cancer, suggesting that BAP1 is a tumor suppressor. However, whether *BAP1* influences the progression of ccRCC tumors expressing wild-type (WT) *BAP1* is unclear. Here, we assessed the expression and function of BAP1 using human ccRCC specimens and cell lines. Analysis of datasets in The Cancer Genome Atlas revealed that lower *BAP1* expression is correlated with longer overall survival of ccRCC patients. We established human ccRCC cell lines with stable *BAP1* knockout and performed multiomic analysis of BAP1-mediated cellular processes. *BAP1* knockout downregulated proteins associated with protein synthesis, resulting in decreased cell growth. Importantly, loss of *BAP1* decreased the formation of stress fibers and membrane protrusions and induced migration and invasion defects. *BAP1* knockout in ccRCC cells also downregulated the expression of transcriptional repressor protein Snail and decreased the activity of Rho family GTPases, promoting the cells to undergo mesenchymal-epithelial transition. Unexpectedly, quantitative proteomics also showed that *BAP1* knockout increased expression of several amino acid transporters and multiple tyrosine kinases, including the epidermal growth factor receptor. Overall, our results suggest that BAP1 regulates multiple cellular processes, and we also uncover a new role for BAP1 in controlling mesenchymal-epithelial transition in ccRCC cells. *Molecular & Cellular Proteomics 18: 1320–1329, 2019. DOI: 10.1074/mcp.RA119.001457.*

BAP1[1] is a member of the ubiquitin C-terminal hydrolase subfamily of deubiquitinating enzymes (DUBs) (1). Histone H2A (Lys119) was the first identified substrate of BAP1 (2); since then, many other targets have been reported, including the transcription factor Krueppel-like factor 5, the cytoskeletal protein γ-tubulin, and the receptor protein IP3R3 (3–5). Calypso, the *Drosophila* orthologue of BAP1, interacts with the additional sex combs protein to form the polycomb-repressive deubiquitinase complex, which is involved in repression of HOX genes during embryo development (2). BAP1 has been shown to interact with several transcription factors and epigenetic modifiers (6), indicating that it plays important roles in transcriptional regulation. Consistent with this, BAP1 is known to be involved in a variety of cellular processes, such as cell cycle progression, endoplasmic reticulum stress response, and DNA repair (7–10).

BAP1 was originally identified as a ubiquitin C-terminal hydrolase that binds to the RING finger domain of BRCA1 and enhances BRCA1-mediated tumor suppressive activity (1). However, BAP1 also exhibits tumor suppressive behavior in a BRCA1-independent manner (11, 12). *BAP1* is located on chromosome 3p21 in a region frequently altered in various cancers, such as mesothelioma and uveal melanoma (13, 14), suggesting that BAP1 is a tumor suppressor. Interestingly, an increasing number of studies have demonstrated that depletion of *BAP1* inhibits the proliferation of various tumorigenic or nontumorigenic cell types (3, 9, 15–17), and germline mutation or low expression of *BAP1* correlates with long-term survival of patients with mesothelioma (18, 19). These results suggest that *BAP1* plays context-specific roles in cancer progression.

Renal cell carcinoma (RCC) is the seventh and ninth most common cancer in men and women, respectively, worldwide. Among the various subtypes, clear cell RCC (ccRCC) is the most common and aggressive subtype, accounting for ~75% of cases (20, 21). Genomic studies have revealed that *BAP1* is mutated in about 10% of ccRCCs, and mutant *BAP1* is associated with poor overall survival in patients with higher Fuhrman grade (22, 23). *BAP1* mutation is also associated with up-regulation of the mammalian target of rapamycin

From the ‡MOE Key Laboratory of Bioinformatics, Center for Synthetic and Systematic Biology, School of Life Sciences; §MOE Key Laboratory for Protein Science, School of Life Sciences, Tsinghua University, Beijing, China; ¶Tsinghua University-Peking University Joint Center for Life Sciences, Beijing, China; ‖Department of Gastroenterology and Hepatology, and Center of Nephrology, Chinese PLA General Hospital, Beijing, China

Received March 26, 2019
Published, MCP Papers in Press, April 16, 2019, DOI 10.1074/mcp.RA119.001457

(mTOR) pathway in ccRCC (22) and has been suggested to be predictive not only for sensitivity to mTOR inhibitors but also for responsiveness to radiotherapy (24). Given the molecular heterogeneity of ccRCC (25, 26), it is equally important to characterize BAP1 function in the ~90% of ccRCC patients carrying WT *BAP1*. Such studies will help to identify molecular diagnostics and possible therapeutic targets for personalized therapy.

To explore the function of BAP1 in ccRCC, we used clustered regularly interspaced short palindromic repeats (CRISPR)-Cas9 technology to knock out *BAP1* in human ccRCC cell lines and performed proteomic and functional analyses. We found that *BAP1* knockout (KO) affected genes involved in cell proliferation, cytoskeletal reorganization, and cell motility. Functional assessment confirmed that *BAP1* KO inhibited the growth, altered the morphology, and reduced the migration and invasion of ccRCC cells. These results provide a comprehensive view of BAP1-mediated cellular processes in ccRCC and reveal that it plays essential roles in cytoskeletal remodeling.

EXPERIMENTAL PROCEDURES

Cell Culture—786-O and 769-P cell lines were obtained from the cell bank of Chinese Academy of Sciences (Shanghai, China). 786-O and 769-P cells were maintained in RPMI 1640 media (Wisent, Nanjing, China, #350–006-CL) supplemented with 10% fetal bovine serum (PAN, Aidenbach, Germany, #ST30–3302) and 1% penicillin/streptomycin (Gibco, Waltham, MA, #15140122) at 37 °C in a humidified incubator with 5% CO_2.

Gene Editing—Genome engineering for creation of *BAP1* null alleles was performed as previously described (27) with modification that dual single-guide RNAs (sgRNAs) were used to achieve high efficiency (28) (guide sequence 1: tagagacctttcgccgggac score:94; guide sequence 2: gggttgtcggtaccgacacc score:95). Briefly, guide sequences were designed by the online tool (http://crispr.mit.edu/) according to the protocol and were cloned into PX458 vector and then transfected into cells with Lipofectamine 3000 (Invitrogen, Waltham, # L3000015) following manufacturer's guidance. 48 h post transfection, cells were trypsinized into single cells and resuspended with PBS, then GFP-positive cells were sorted into 96-well plates by FACSAria™II flow cytometer (BD) in a single-cell mode. 10–14 days after sorting, visible monoclones were submitted to PCR genotyping (primer-up: tgagtgatgacgcagtgcaaaggat; primer-down: tggagaccaagacaaggaatcagcg) and then validated by Western blotting.

Experimental Design and Statistical Rationale—Quantitative proteomic profiling was performed on three independent biological replicates. 786-O *BAP1* knockout and WT cells were used as experimental and control cell lines, respectively. To minimize the variability between samples, Tandem Mass Tag labeling was used to obtain accurate quantitative information. For quantitative analysis, at least two unique peptides were considered for the identification and quantification of proteins. To minimize experimental bias or errors and based on the assumption that the majority of the proteins do not or just slightly changed between samples, the reporter ion abundance was normalized to total peptide amount so that the total abundance is the same for all channels. The normalized abundances from each channel were used to calculate the mean ratios of identified proteins, and Student's *t* test was used to verify the significance of the results. Significantly changed proteins were screened by volcano plot analysis using R (V.3.5.1). Histograms of protein fold-changes in proteomic data were used to demonstrate normal data distribution. Pearson correlation was calculated to test the reproducibility of protein quantification.

Sample Preparation—Cells were lysed with 8 M urea supplemented with protease inhibitor mixture (Bimake, Shanghai, China, #B14002), 100 μg of protein were reduced with 5 mM DTT for 60 min at room temperature and alkylated with 12 mM iodoacetamide for 45 min at room temperature in the dark. Samples were then digested with trypsin (Promega, Madison, # V5280) at 37 °C overnight. The peptides were desalted with Sep-Pak C18 Cartridge (Waters, Milford, # 186004619) and labeled with Tandem Mass Tag (ThermoFisher, Waltham, MA) following manufacturer's instructions. The labeled peptides of different samples were mixed, desalted, and separated by high performance liquid chromatography (HPLC) into 12 fractions at pH 10 and then analyzed by LC-MS/MS.

LC-MS/MS Analysis—For LC-MS/MS analysis, each fraction was separated by HPLC (Ultimate 3000, ThermoFisher) in a 135-min gradient elution with 0.1% formic acid, which was connected to a Thermo Orbitrap Fusion Lumos mass spectrometer. The mass spectrometer was programmed to acquire in the data-dependent acquisition mode. The master scan was from 350 to 1,550 *m/z* with a resolution of 120K at 400 *m/z*, and the duty cycle was 3 s. After one master scan, the top *N* most intense peaks with charge state 2 and above were dissociated by normalized collision energy of 35% (27% for stable isotope labeling with amino acids in cell culture (SILAC) samples) with an isolation window of 0.7 Da width, and the dynamic exclusion duration was 15 s. The MS2 spectra were acquired with a resolution of 30K, automatic gain control (AGC) target of 2×10^5, and maximum injection time of 60 ms.

Protein Identification and Quantification—The MS/MS spectra were searched against the UniProt human database (release on October 25, 2017, containing 20,168 entries) using the SEQUEST search engine of Proteome Discoverer 2.1 software (ThermoScientific). The search criteria were as follows: full tryptic specificity was required, two missed cleavage was allowed, carbamidomethylation on cysteine and Tandem Mass Tag sixplex on lysine/peptide N terminus were set as the fixed modifications, oxidation on methionine and acetylation on protein N terminus were set as the variable modification, precursor ion mass tolerances were set at 10 ppm, and the fragment ion mass tolerance was set to 0.02 Da. Peptide spectral matches were validated using the Percolator provided by Proteome Discoverer software at a 1% false discovery rate. The reporter ion abundance was normalized to total peptide amount, and abundance from each channel was used to calculate the mean ratio of identified proteins.

Identification of Ubiquitinated Proteins—786-O WT and *BAP1* KO cells were cultured in heavy ($^{13}C_6$-L-arginine, $^{13}C_6$-L-lysine, Cambridge Isotope Lab, Cambridge, UK) and light (unlabeled L-arginine and L-lysine) SILAC RPMI 1640 medium (Thermo Fisher Scientific), respectively. After more than 10 passages, cells were lysed with 8 M urea and 5 mg protein from each group were mixed. The ubiquitinated peptide enrichment was performed using PTMScan® (Cell Signaling Technology, Boston, MA, #5562) following the manufacturer's instructions. Briefly, the sample was reduced with 5 mM DTT for 60 min at room temperature and alkylated with 12 mM iodoacetic acid for 45 min at room temperature in the dark. Samples were then digested with trypsin (Promega) at 37 °C overnight. The peptides were desalted with Sep-Pak C18 Cartridge (Waters) and lyophilized. The peptides were dissolved in immunoaffinity purification (IAP) buffer and

[1] The abbreviations used are: BAP1, BRCA1-associated protein 1; ccRCC, clear cell renal cell carcinoma; BRCA1, breast cancer type 1 susceptibility protein; IP3R3, inositol 1,4,5-trisphosphate receptor type 3; SETD2, histone-lysine N-methyltransferase SETD2; KDM5C, lysine-specific demethylase 5C; EMT, epithelial–mesenchymal transition.

incubated with motif antibody beads for 2 h at 4 °C. Then the beads were washed by IAP buffer for two times and PBS for two times and eluted by 0.15% TFA. The sample was desalted by home-made C18 stage-tips for LC-MS/MS analysis. The LC-MS/MS and search criteria were the same as described above with changes: (1) 13C(6) at lysine, ubiquitination at lysine, 13C(6)+ubiquitination at lysine, and 13C(6) at arginine were set as variable modifications and carboxymethylation on cysteine was set as fixed modifications (carbamidomethylation and Tandem Mass Tag modification were removed); (2) relative peptide expression ratios were calculated using the precursor ion intensity of Lys0Arg0 and Lys6Arg6.

RNA Sequencing—Total RNA was extracted with RNAprep kit (TIANGEN, Beijing, China, #DP430) and the quality of RNA was checked by 2100 bioanalyzer (Agilent, Palo Alto, CA), samples have the RNA Integrity Number (RIN) value that higher than 7 can be used for sequencing. For library preparation, KAPA mRNA HyperPrep Kit (Roche, Basel, Switzerland, # KK8581) was used following manufacturer's instructions. Then the library quality was checked by a 2100 bioanalyzer and quantified by Qubit (ThermoFisher). Illumina Hiseq X-TEN platform was used for sequencing.

Rho Activity Assay—The activities of RhoA, Rac, and Cdc42 were determined as previously described (29). GST-Rhotekin-RBD and GST-PAK-RBD were prepared in-house. Cells were lysed with radioimmune precipitation assay buffer supplemented with protease inhibitor mixture (bimake) for 2 h at 4 °C. 100 μg of lysate of each cell type were incubated with GST-Rhotekin-RBD (for GTP-RhoA assay) or GST-PAK-RBD (for GTP-Rac and GTP-Cdc42 assay) prebound GSH-Sepharose beads (GE Healthcare, Boston, # 17075604) for 2 h at 4 °C. Then the beads were washed by PBS and boiled with 50 μl of loading buffer for 5 min. The eluted proteins were submitted to Western blot analysis.

Western Blotting—Cells were lysed with radioimmune precipitation assay buffer supplemented with protease inhibitor mixture and sonicated. After centrifugation at 14,000 $\times$ *g* for 15 min at 4 °C, the supernatant was collected. The protein concentration was measured by BCA assay kit. Equal amount of proteins was separated by 12% SDS-PAGE gel and transferred onto a PVDF membrane. After block with 5% milk for 1 h, the membrane was incubated with primary antibody overnight at 4 °C then incubated with secondary antibody conjugated with HRP for 1 h. The membrane was detected by ECL reagents (GenStar, Beijing, China, #E171–04) with Image Lab system (Bio-Rad, Hercules). BAP1 antibody (#sc-28383) was purchased from Santa Cruz; H2AUbi (#8240), H2A (#12349), beta-actin (#4970), Rac (#2465), RhoA (#2117), Cdc42 (#2466), Snail (#3879), N-cadherin (#13116), and vimentin (#5741) antibodies were purchased form Cell Signaling Technology.

Quantitative Real-time PCR—Total RNA was extracted by RNAprep kit (TIANGEN, #DP430) and reverse transcribed to cDNA by GoScript™ system (Promega, #A5001) according to manufacturer's instructions. Real-time PCR was performed by LightCycler™ 480II (Roche, Switzerland) with SYBR green qPCR mix (Takara, Dalian, China, #RR390A), 18s rRNA was used as internal control. Relative expression level was calculated by double delta Ct analysis. Primers used for qPCR were listed in Table S3.

Wound Healing Assay—Cells were counted and seeded in 12-well plates (2×10^5 per well) overnight before experiment. Two cross wounds were made in each well with a sterile tip. Then the cells were rinsed several times with PBS and then culture media. Pictures were taken by Eclipse Ts2 (Nikon, Tokyo, Japan) at indicated time point.

Transwell Assay—Transwell 24-well permeable supports (Corning, Coring, #3422) were used. The upper surface of the inserts (6.5 mm diameter) were coated with 0.5 mg/ml rat tail collagen (Corning, Coring, #354236) for 2 h before use. 3×10^4 cells were counted and seeded in the inserts with RPMI 1640 without FBS, and the lower chambers were filled with RPMI 1640 containing 10% FBS. After 12 h, the upper surface of the inserts were cleaned and the invasive cells on the lower surface were fixed with 4% paraformaldehyde and stained with crystal violet solution (Beyotime, Shanghai, China, #C0121). The number of invasive cells were calculated with three areas (up, middle, and down) on the lower surface of inserts.

Chromatin Immunoprecipitation (ChIP) Analysis—ChIP assay was performed following the ChIP protocol from Cold Spring Harbor (30). Briefly, 786-O WT and *BAP1* KO cells were harvested and fixed with 1% formaldehyde/PBS for 10 min at room temperature. Nuclei were extracted and lysed, and the chromatins were sonicated into fragments with an average length of 0.3–0.5 kb. Chromatins were incubated with E6C5 antibody (mouse IgM, Merck Millipore, Darmstadt, Germany, #05–678) at 4 °C overnight, and then incubated with second antibody (rabbit anti-mouse IgM, Merck Millipore, #12–488)-preconjugated protein A dynabeads (Invitrogen, #10001D) at 4 °C overnight. Input and purified immunoprecipitated DNA were quantified by real-time PCR. Primers used for ChIP-qPCR were listed in Table S3.

Phalloidin Staining—Cells were plated on a 35-mm glass bottom cell culture dishes (NEST, Wuxi, China). After 24 h, cells were washed in PBS, fixed with 4% paraformaldehyde for 10 min, permeabilized with 0.1% Triton X-100 for 5 min, washed in PBS, and then stained with phalloidin-TRITC (1:200, YEASEN, Shanghai, China, #40734ES75) in 1% BSA for 30 min at 4 °C, washed in PBS and then stained with DAPI staining solution (Beyotime, #C1006). The dishes were mounted with antifading mounting medium (Solarbio, Beijing, China, #S2100). Images were captured by Nikon A1 Laser Scanning Confocal Microscopy and then analyzed by ImageJ software.

Dual-luciferase Assay—The *Snail* promoter was synthesized and cloned into pGL3-Basic vector. 293T cells were plated in 24-well plates overnight. pcDNA3.1-BAP1 or empty pcDNA3.1 was co-transfected into 293T with Renilla and pGL3-*Snail*-promopter. 48 h post transfection, luciferase activity was measured by using the dual luciferase reporter assay system (Promega) following the manufacturer's instructions. The experiments were repeated in triplicate with normalization to Renilla activity.

Cell Proliferation Assay—Cells were counted and seeded in 96-well plates (2,500 cells per well). Cell proliferation rate was measured by Cell Counting Kit-8 (Dojindo, Kyushu, Japan, # CK04) according to the manufacturer's guidance. Optical density at 450 nm was measured with a microplate reader (ThermoFisher) after incubation with Cell Counting Kit-8 for 2 h.

Statistical Analysis—Data plotting and statistical analysis were carried out with SigmaPlot software. Data are presented as mean $\pm$ S.D. $n = 3$. Student's *t* test was used to determine the significance, and *p* values lower than 0.05 were considered to be significant. A Kaplan-Meier survival curve was plotted by GraphPad Prism 6 software, and the raw data were downloaded from OncoLnc online tool (31) and listed in Table S2. For the analysis, 33% of the upper and lower percentile were used.

RESULTS

Low BAP1 Expression Correlates With Longer Overall Survival in ccRCC Patients—To determine whether expression of WT *BAP1* correlates with the survival of ccRCC patients, we analyzed genomic datasets from two cohorts (32) in The Cancer Genome Atlas. Among these, 89.62% (380 of 424) and 90.69% (409 of 451) of the patients expressed WT *BAP1* (Fig. 1*A*). Using the OncoLnc data analysis tool, we found that lower *BAP1* mRNA expression levels correlated with longer

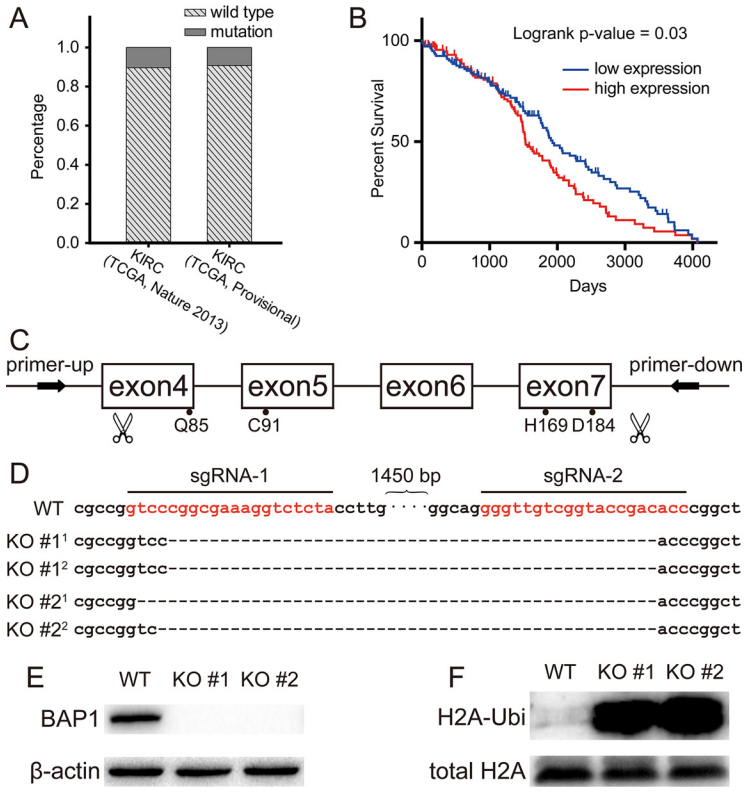

FIG. 1. **Low expression of *BAP1* was correlated with better survival in ccRCC patients.** (*A*) Analysis of genomic datasets from TCGA showed that about 90% of ccRCC patients do not harbor *BAP1* mutation. (*B*) Lower *BAP1* mRNA expression levels correlated with longer overall survival within patients carrying WT *BAP1* (n = 133 each in low and high groups). (*C*) Schematic diagram of *BAP1* engineering site for CRISPR-Cas9 and binding site for genotyping primers on genome. (*D*) The CRISPR-Cas9-derived mutations in 786-O *BAP1*-KO #1 and KO #2 cells were sequenced by Sanger sequencing. (*E*) Validation of endogenous BAP1 by Western blotting in *BAP1* WT and KO cells. (*F*) Verifying the increase of ubiquitination on lysine119 of histone H2A by Western blotting.

overall survival within patients carrying WT *BAP1* (Fig. 1*B*). This result suggested that *BAP1* may play complex roles in tumor progression other than a tumor suppressor.

To investigate the function of *BAP1* in ccRCC progression, we used CRISPR-Cas9 technology with dual sgRNAs to knock out *BAP1* in the human 786-O and 769-P ccRCC cell lines with high efficiency. The catalytic region of BAP1 includes four crucial amino acids (glutamine 85, cysteine 91, histidine 169, and aspartic acid 184), in which cysteine 91 is the active site (1). Therefore, we designed two sgRNAs to flank this domain and designed genotyping primers to flank the sgRNAs (Fig. 1*C*). *BAP1* KO was confirmed by Sanger sequencing. As shown in Fig. 1*D*, about 1,500 bp was deleted in both alleles of *BAP1* to generate two stable KO cell monoclones. *BAP1* KO was also subsequently confirmed by Western blot analysis (Fig. 1*E*).

Proteomic Analysis Showed That BAP1 was Involved in Cytoskeleton Remodeling and Cell Growth in ccRCC Cells—H2A is a canonical substrate of BAP1 (2). Western blot analysis showed that H2A ubiquitination was significantly increased in *BAP1* KO 786-O cells compared with the control cells (Fig. 1*F*), indicating that BAP1 epigenetically regulates gene expression in these cells. Because BAP1 is a deubiquitinating enzyme, we probed changes in the ubiquitome of *BAP1* KO cells compared with WT cells. Gene Ontology analysis of proteins with increased ubiquitination in KO cells showed that BAP1 participated in RNA processing, translation, and chromatin remodeling in 786-O cells (Fig. S1).

Next, we performed quantitative proteomic analysis to explore the effects of *BAP1* KO on proteostasis in ccRCC cells. In triplicate samples, we identified 7,738 proteins, of which 1,469 were classified as differentially expressed proteins (DEPs; Table S1) according to the following criteria: (1) false discovery rate of protein <0.01, (2) average reporter ion ratio >1.3 or <0.77, (3) p value of the ratio <0.05, and (4) identification of two or more unique peptides. Histograms showed normal Gaussian distributions of fold-changes from proteomic data (Fig. 2*A*). A high Pearson correlation coefficient indicated high correlation in fold-changes among three biological replicates (Fig. 2*A*). The cutoff ratio for up- or down-regulated proteins was determined using a biological replicate method (33). Applying this method to our data, we observed about 25% variation corresponding to 88% coverage of data (Fig. 2*B*). Based on this, the cutoff was set at 1.3-fold ($1 \pm 30\%$ variation). In the volcano plot, blue dots in the upper left and red dots in the upper right sections represent proteins with fold-change < 0.77 or > 1.3 and p values < 0.05 (Fig. 2*C*).

Gene Ontology enrichment analysis was then performed to determine the biological relevance of the DEPs. The most highly enriched Molecular Function terms for the DEPs were Binding and Catalytic Activity (Fig. S2), especially Cytoskeletal Protein Binding and Motor Activity (Fig. 3*A*). Totally, 130 cytoskeleton binding proteins and 12 motor proteins were enriched (marked in Table S1), which indicated that BAP1 was involved in cytoskeleton remodeling and cell motility. To gain

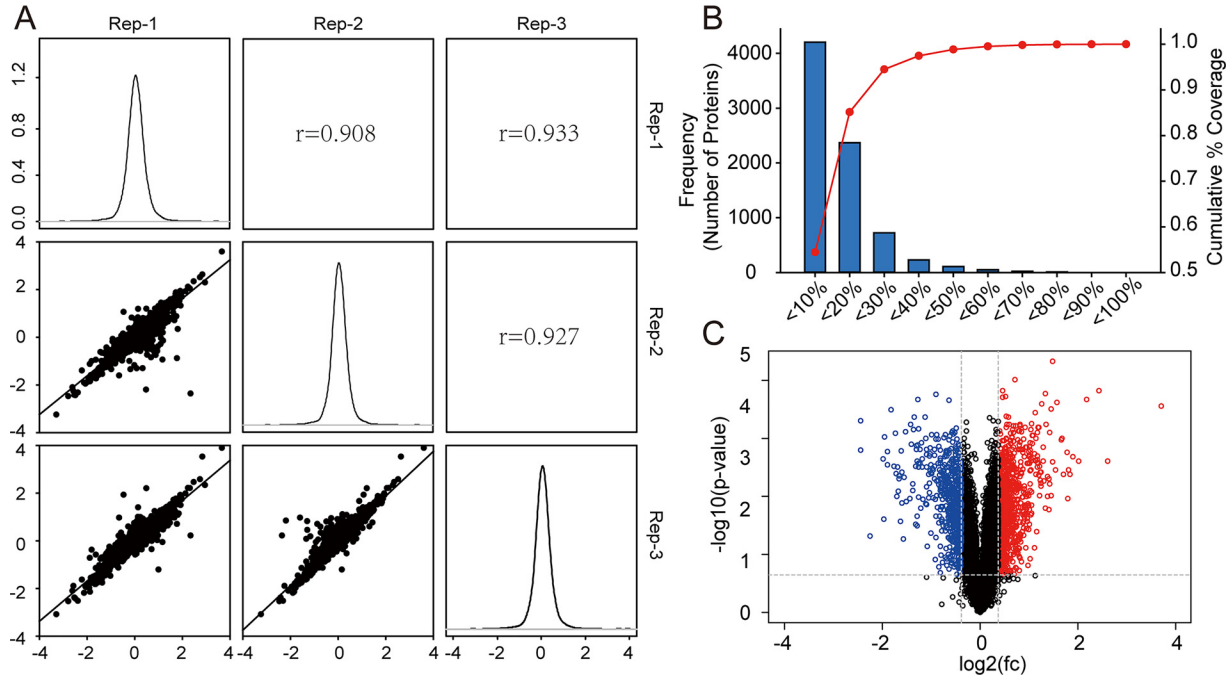

FIG. 2. **Quantitative proteomic analysis of 786-O *BAP1* KO cells and WT cells.** (*A*) Histograms showed normal Gaussian distributions of log2(fold change) from proteomic data and high Pearson correlation coefficient indicated high correlation in fold-changes among three biological replicates. (*B*) About 25% variation corresponded to 88% coverage of the proteomic data, and based on this, the cutoff was set at 1.3 fold (1 ± 30% variation). (*C*) Volcano plots showed significantly changed proteins in *BAP1* KO cells with fold-change > 1.3 (labeled in red) or < 0.7 (labeled in blue) and *p* value < 0.05.

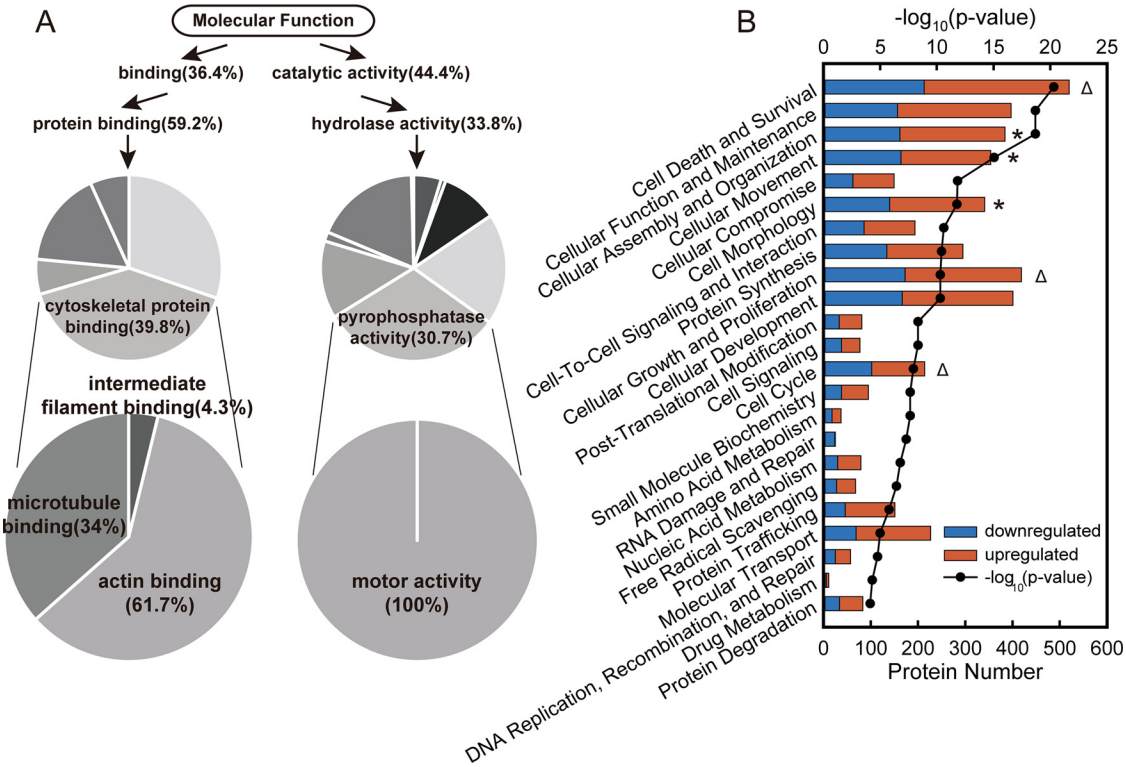

FIG. 3. **GO analysis of differentially expressed proteins between 786-O *BAP1* KO cells and WT cells.** (*A*) Cytoskeleton and motor related proteins were highly enriched within DEPs using Molecular Function enrichment with PANTHER bioinformatics platform. (*B*) Cellular processes enriched by Ingenuity Pathway Analysis software showed that BAP1 was significantly involved in cell morphology and mobility (indicated by *) and cell proliferation (indicated by Δ).

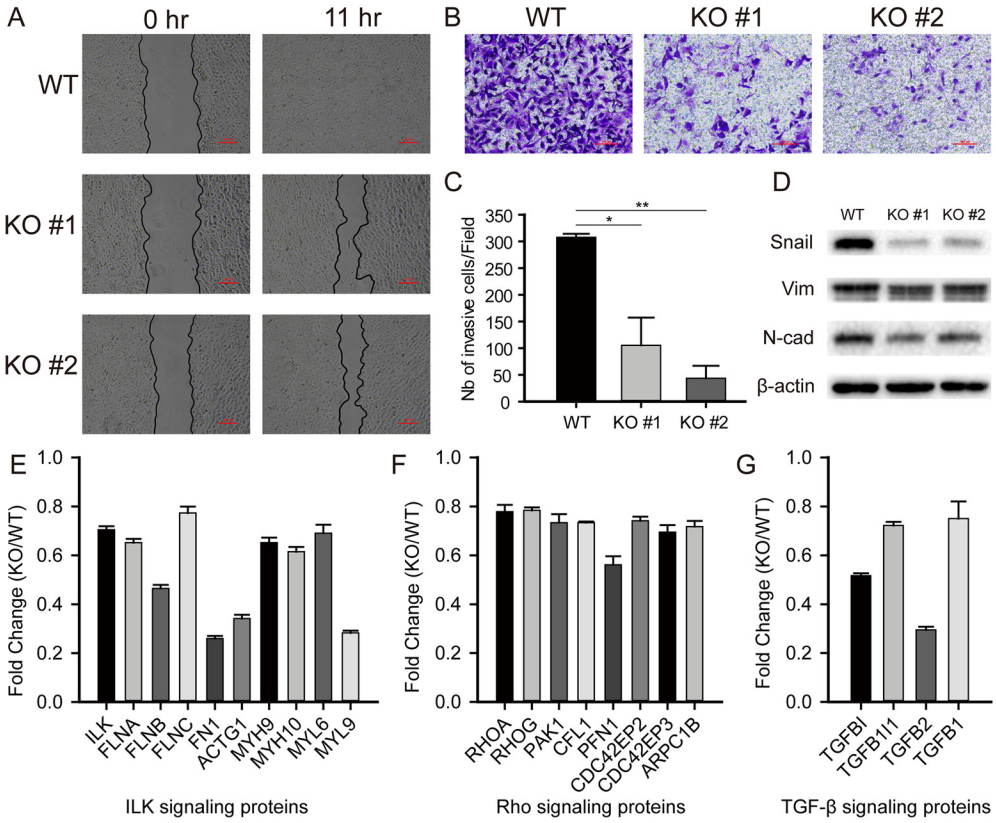

FIG. 4. **Loss of *BAP1* promoted mesenchymal-epithelial transition in 786-O ccRCC cells.** (*A*) Representative images of wound-healing assay showed that loss of *BAP1* inhibited cell migration. Scale bar: 200 μm, $n = 3$. (*B*) Representative images of Transwell assay showed that *BAP1* KO induced invasion defect. Scale bar: 100 μm, $n = 3$. (*C*) Bar graphs based on quantitative data from panel B, $n = 3$. (*D*) Western blot analysis quantifying makers related to epithelial-mesenchymal transition, $n = 3$. (*E–G*). Proteomic analysis showed downregulated proteins associated to EMT process in *BAP1* KO cells. $^{*}p < 0.05$; $^{**}p < 0.01$; $^{***}p < 0.001$.

further insight, we subjected the DEPs to ingenuity pathway analysis (IPA) and found that proteins related to cell morphology and motility (* in Fig. 3*B*) and cell proliferation (Δ in Fig. 3*B*) were highly enriched. Cell morphology and motility networks were represented by cellular assembly and organization, and cellular movement and cell morphology. Cell proliferation was represented by cell death and survival, cellular growth and proliferation, and cell cycle. In total, 576 DEPs were related to cell morphology and motility, and 683 were related to cell proliferation. Among the proteins downregulated by *BAP1* KO were filamins, which promote actin filament branching; myosins, which are responsible for cell contraction; and fibronectin, a matrix protein that plays a key role in wound healing. Canonical pathways related to cell morphology and motility were also significantly enriched in the IPA (Fig. S3). Similar results were observed from analysis of RNA-seq data (Fig. S4). All these results suggested that BAP1 played a crucial role in regulation of cell motility and cytoskeletal reorganization.

BAP1 KO Downregulates Snail Expression to Promote the Mesenchymal-epithelial Transition (MET) in ccRCC Cells—We next examined the effects of *BAP1* KO on cell migration in more detail using a wound-healing assay. While migration of *BAP1* WT cells effectively closed the wound within 11 h of incubation, the migration of *BAP1* KO cells was much slower (Fig. 4*A*). Similar results were obtained with the 769-P ccRCC cell line (Fig. S5*A*). Next, we examined the effects of *BAP1* KO on invasive behavior using a Transwell assay with collagen-coated wells. After 12-h incubation, the number of invaded *BAP1* KO cells was much lower than that of the WT cells (Figs. 4*B* and 4*C*). These results demonstrated that BAP1 plays an important role in the migratory and invasive behavior of ccRCC cells.

The observed reduction in ccRCC cell motility suggested that BAP1 might be involved in the EMT and/or the reverse process MET, which are crucial not only for embryonic development but also for the progression of tumors (34, 35). While the EMT promotes tumor invasion and initiates metastasis, metastatic cells may undergo MET to form new colonies (metastases), which are responsible for ~90% of deaths from cancer in humans (36, 37). The transcription factor Snail plays a key role in these processes by regulating the expression of several EMT- and MET-related proteins, such as E-cadherin, vimentin, and fibronectin (38). Consistent with the results of the migration and invasion assays, Western blot analysis of ccRCC cells showed a pronounced decrease in the expression of Snail, N-cadherin, and vimentin in *BAP1* KO cells compared with WT cells (Fig. 4*D*), which suggests a role for

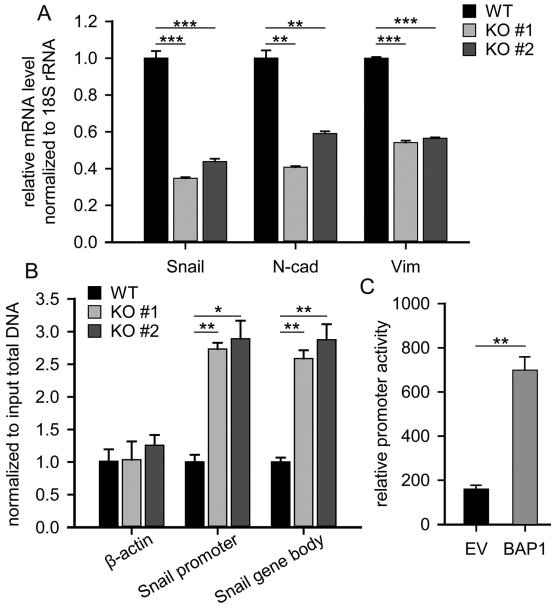

FIG. 5. **BAP1 regulated the transcription of *Snail* through deubiquitinating H2A.** (*A*) Quantitative real-time PCR quantifying the mRNA level of EMT markers, $n = 3$. (*B*) ChIP analysis showed that H2Aub (Lys119) modification was highly enriched on *Snail* gene but not on *β-actin* gene, $n = 3$. (*C*) Dual-luciferase assay showed that BAP1-enhanced *Snail* promoter activity by about fourfold compared with control empty vector, $n = 3$. $^{*}p < 0.05$; $^{**}p < 0.01$; $^{***}p < 0.001$.

BAP1 in coordinating the EMT process. Proteomic data also showed that proteins associated with integrin-linked protein kinase-, ras homolog-, and transforming growth factor beta-signaling pathways were significantly downregulated in *BAP1* KO cells (Figs. 4*E*–4*G*).

Because BAP1 deubiquitnates H2A on Lys119, which is an epigenetic marker implicated in transcription repression (39, 40), we hypothesized that BAP1 regulated *Snail* expression at the transcription level. To verify this, real-time PCR assay was performed and the result confirmed that *Snail* mRNA was significantly downregulated in *BAP1* KO cells (Fig. 5*A*). In addition, ChIP analysis showed that H2Aub (Lys119) was highly enriched in the *Snail* but not *β-actin* gene region (Fig. 5*B*). Further, we performed dual-luciferase reporter assays in which firefly luciferase expression was driven by *Snail* promoter activity. Indeed, luciferase activity was fourfold higher in 293T cells transfected with the pcDNA3.1-BAP1 expression vector compared with the control empty vector (Fig. 5*C*), which confirmed that BAP1 directly regulated *Snail*-promoter activity. Collectively, these results suggested that BAP1 directly regulates *Snail* mRNA levels by deubiquitinating H2A in the *Snail* gene region and that loss of *BAP1* in 786-O cells induced MET by inhibiting *Snail* expression.

Loss of BAP1 Decreases Rho Activity and Induces Morphological Changes in ccRCC Cells—To further probe the mechanism by which BAP1 regulates the migration and invasion of ccRCC cells, we examined cytoskeletal organization in *BAP1* KO and WT cells using the fluorescent F-actin-binding protein phalloidin. As shown in Fig. 6, cells with *BAP1* KO exhibited smooth margins, decreased formation of stress fibers, disordered actin alignment, and reduced pseudopodia (Fig. 6*A* and insets). The Rho family GTPases (Rho, Rac, and Cdc42) are key regulators of cytoskeletal organization and play crucial roles in cell adhesion and movement. Rho participates in the formation of stress fibers and modulates cell morphology and motility; Rac regulates actin polymerization and cell-cell adhesion; and Cdc42 is involved in filopodia formation and cell-cell adhesion (41). During cell migration, Cdc42 determines the direction of cell movement, Rac and Cdc42 induce actin-rich membrane protrusions at the leading edge, and Rho promotes actin-myosin contractility for forward movement (42). Consistent with these functions and the observed effects of *BAP1* KO on ccRCC cell morphology and motility, GTPase activity assays showed that RhoA, Rac, and Cdc42 activities were all significantly downregulated in *BAP1* KO cells compared with WT cells (Fig. 6*B*). Interestingly, Western blotting and quantitative real-time PCR analysis showed that total protein and mRNA levels of each Rho family member were downregulated, indicating that BAP1 regulates their expression at the mRNA level (Fig. 6*C*). Several studies have demonstrated that Snail regulates cell motility through modulating the expression and activity of Rho family GTPases (43–46). As described above, loss of *BAP1* directly downregulated the expression of *Snail*, and this should result in the decreased expression and activity of Rho family GTPases, subsequently. Importantly, the reduction in stress fiber and pseudopodia formation and GTPase activities induced by loss of *BAP1* was observed in both 786-O and 769-P (Fig. S6) cell lines.

Loss of BAP1 Inhibits ccRCC Cell Growth—Because a large number of the proteins differentially expressed in *BAP1* KO cells were involved in cellular processes related to cell proliferation (683 DEPs), we examined cell proliferation using the Cell Counting Kit-8 assay. Indeed, loss of *BAP1* decreased the growth of both 786-O and 769-P (Fig. 7*A* and Fig. S7) cells. Because proteomic analysis revealed a significant down-regulation of 28 ribosomal subunits in *BAP1* KO cells (Fig. 7*B*), it seems likely that the observed growth inhibition of these cells was at least partly due to decreased protein synthesis. To determine whether *BAP1* KO affected cell cycle progression, we performed FACS analysis of ccRCC cells stained with the DNA-intercalating dye propidium iodide. Cell cycle analysis showed that *BAP1* KO in 786-O cells induced S-phase arrest (Fig. 7*C*), consistent with an earlier report that shRNA-mediated *BAP1* knockdown slowed S-phase progression in HeLa cells (17).

Paradoxically, we also found that *BAP1* KO up-regulated several growth-promoting transporters and growth factors/receptors in ccRCC cells. These included transporters of amino acids (SLC3A2, SLC7A5, SLC7A1, SLC25A15, and SLC15A4) and monocarboxylates (SLC16A1), epidermal growth factor receptor, fibroblast growth factor 2, and hep-

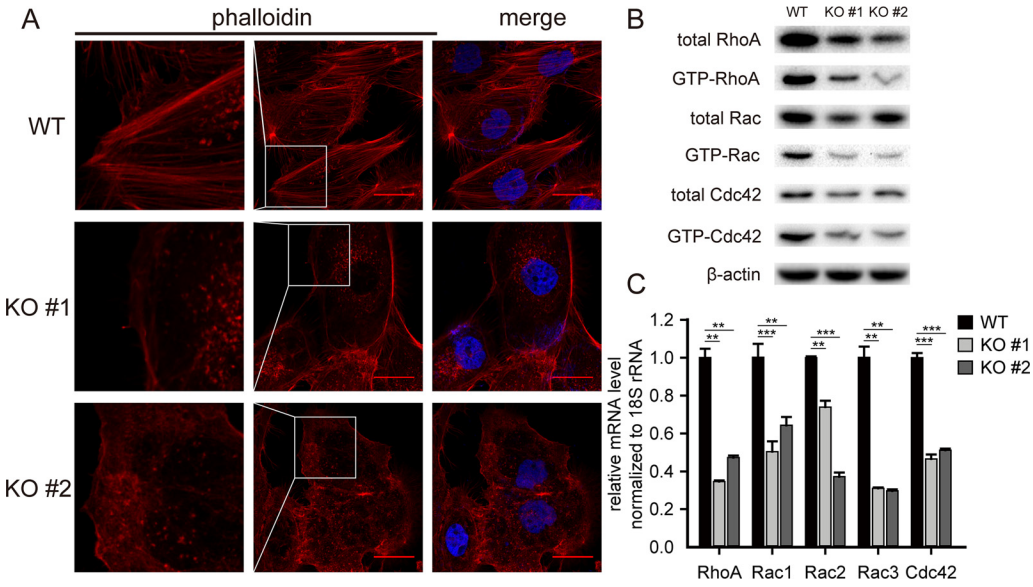

FIG. 6. ***BAP1* knockout decreased the formation of stress fibers and membrane protrusions in 786-O ccRCC cells.** (*A*) Staining of 786-O cells with TRITC-phalloidin (red) to observe F-actin fibers. *BAP1* KO cells exhibited smooth margins and decreased formation of stress fibers, with disordered actin alignment and reduced pseudopodia. Scale bar: 25 μm, $n = 3$. (*B*) Western blotting quantifying the total and active form of Rho family GTPases in 786-O WT and KO cells, $n = 3$. (*C*) Quantitative real-time PCR quantifying the mRNA level of Rho family GTPases in 786-O WT and KO cells, $n = 3$. $^{**}p < 0.01$; $^{***}p < 0.001$.

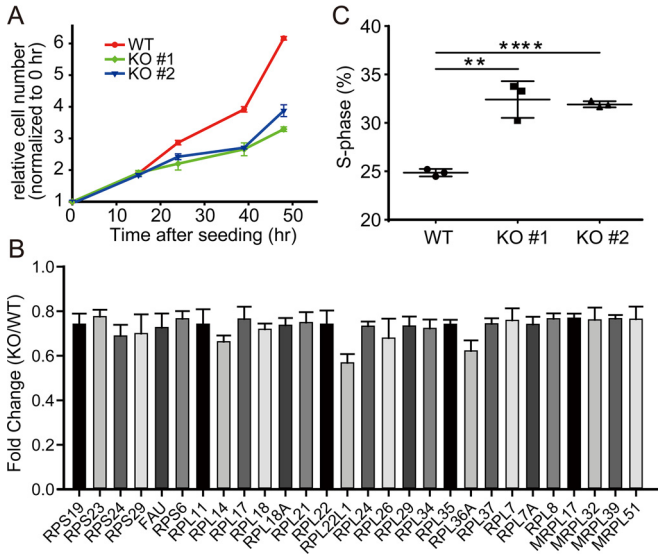

FIG. 7. ***BAP1* knockout inhibited cell proliferation in 786-O ccRCC cells.** (*A*) Loss of *BAP1* inhibited cell proliferation in 786-O cells, $n = 3$. (*B*) Proteomic analysis showed downregulated subunits of cytosolic and mitochondrial ribosomes in 786-O *BAP1* KO cells. (*C*) Loss of *BAP1* induced S-phase cell cycle retardation in 786-O *BAP1* KO cells.

atocyte growth factor receptor (Fig. S8). This observation suggested that BAP1 plays complex roles in cell growth regulation.

DISCUSSION

Next-generation sequencing studies have shown that epigenetic modifiers such as protein polybromo-1, SETD2, BAP1, and KDM5C are frequently mutated in RCC and other tumors (13, 25, 47–49). These proteins are involved in regulating diverse cellular processes, including DNA repair, cytoskeletal remodeling, and transcription (47). Previous studies have proposed that BAP1 functions as a tumor suppressor (1, 11), but accumulating evidence suggests that it also plays a role in promoting cell proliferation (9, 10, 15). *BAP1* is estimated to be mutated in about 10% of ccRCC cases. In the present study, we found that lower expression of WT *BAP1* in ccRCC correlated with longer overall survival, suggesting that BAP1 played complex roles in ccRCC other than just a tumor suppressor. Ubiquitomic analysis showed that BAP1 was associated with multilevel regulation of gene expression. Our quantitative proteomic analysis revealed that *BAP1* KO altered proteostasis in ccRCC cells, especially the expression of proteins associated with cell motility, cytoskeletal organization, and cell proliferation. These properties were confirmed by functional assays of ccRCC cell motility and invasion. The EMT markers Snail, N-cadherin, and vimentin were downregulated in *BAP1* KO cells, and importantly, we demonstrated that BAP1 regulates *Snail* transcription by directly deubiquitinating H2A in the *Snail* gene region. Consistent with an MET phenotype, the activities of RhoA, Rac, and Cdc42 GTPases were all significantly decreased by *BAP1* KO, resulting in a striking loss of stress fiber and pseudopodia formation.

The observed suppression of cell growth in *BAP1* KO ccRCC cells could be at least partially attributed to a decrease in protein synthesis. Previous work has identified cytochrome c oxidase subunit 7C (COX7C), a subunit of the mitochondrial

respiratory chain complex cytochrome c oxidase IV, as a BAP1-activated gene (50). Consistent with this, we found that *BAP1* KO in ccRCC cells reduced COX7C expression by three fold compared with *BAP1* WT cells (Table S1). Interestingly, both protein and mRNA level of the immunosuppressive protein programmed death-ligand 1 (PD-L1) were also down-regulated in *BAP1* KO 786-O cells (data not shown). Previous studies have shown that PD-L1 is expressed in 70% of ccRCC tumors (51, 52) and that EMT is linked to $CD8^+$ T cell immunosuppression via up-regulation of PD-L1 (53). Thus, the results presented here point to a possible role for BAP1 in immunosuppression.

In summary, we have demonstrated that inactivation of *BAP1* in ccRCC cells altered cellular proteostasis, suppressed cell proliferation, and induced a MET-like phenotype. Importantly, Snail and Rho family GTPases played fundamental roles in the biological processes regulated by BAP1. Our results also suggested that BAP1 played context-dependent roles in tumor progression.

Acknowledgments—We thank the Protein Chemistry Facility at the Center for Biomedical Analysis of Tsinghua University for sample analysis. We thank WeiKun Xia for the help with gene editing. We thank Anne M. O'Rourke, Ph.D., for editing the English text of a draft of this manuscript.

DATA AVAILABILITY

The proteomic data have been deposited to the ProteomeXchange Consortium via the PRoteomics IDEntifications (PRIDE) partner repository with the dataset identifier PXD012288, PXD013127.

* This work was supported by the National Key Research and Development Program of China (Grant 2017YFA0505103), NSFC (21877068 and 81802519), the Chinese Ministry of Science and Technology (2017ZX10201101 and 2014CBA02005), and the China Postdoctoral Science Foundation (2017M610080).

S This article contains supplemental material Tables S1–S3 and Figs. S1–S8.

** To whom correspondence should be addressed: School of Life Sciences, Tsinghua University, Beijing, 100084, China, Tel: 8610-62790498; Fax: 8610-62797154; Email: dht@tsinghua.edu.cn.

Author contributions: P.C. and H.D. designed research; P.C. and H.W. performed research; P.C., H.W., and W.Z. analyzed data; P.C. and H.D. wrote the paper; Y.C. acquisition of funding; and Y.L., D.W., and M.G. involved in the discussion.

REFERENCES

1. Jensen, D. E., Proctor, M., Marquis, S. T., Gardner, H. P., Ha, S. I., Chodosh, L. A., Ishov, A. M., Tommerup, N., Vissing, H., Sekido, Y., Minna, J., Borodovsky, A., Schultz, D. C., Wilkinson, K. D., Maul, G. G., Barlev, N., Berger, S. L., Prendergast, G. C., and Rauscher, F. J., 3rd. (1998) BAP1: A novel ubiquitin hydrolase which binds to the BRCA1 RING finger and enhances BRCA1-mediated cell growth suppression. *Oncogene* **16,** 1097–1112
2. Scheuermann, J. C., de Ayala Alonso, A. G., Oktaba, K., Ly-Hartig, N., McGinty, R. K., Fraterman, S., Wilm, M., Muir, T. W., and Müller, J. (2010) Histone H2A deubiquitinase activity of the Polycomb repressive complex PR-DUB. *Nature* **465,** 243–247
3. Qin, J., Zhou, Z., Chen, W., Wang, C., Zhang, H., Ge, G., Shao, M., You, D., Fan, Z., Xia, H., Liu, R., and Chen, C. (2015) BAP1 promotes breast cancer cell proliferation and metastasis by deubiquitinating KLF5. *Nat. Commun.* **6,** 8471
4. Bononi, A., Giorgi, C., Patergnani, S., Larson, D., Verbruggen, K., Tanji, M., Pellegrini, L., Signorato, V., Olivetto, F., Pastorino, S., Nasu, M., Napolitano, A., Gaudino, G., Morris, P., Sakamoto, G., Ferris, L. K., Danese, A., Raimondi, A., Tacchetti, C., Kuchay, S., Pass, H. I., Affar, E. B., Yang, H., Pinton, P., and Carbone, M. (2017) BAP1 regulates IP3R3-mediated Ca2+ flux to mitochondria suppressing cell transformation. *Nature* **546,** 549–553
5. Zarrizi, R., Menard, J. A., Belting, M., and Massoumi, R. (2014) Deubiquitination of gamma-tubulin by BAP1 prevents chromosome instability in breast cancer cells. *Cancer Res.* **74,** 6499–6508
6. Carbone, M., Yang, H., Pass, H. I., Krausz, T., Testa, J. R., and Gaudino, G. (2013) BAP1 and cancer. *Nat. Rev. Cancer* **13,** 153–159
7. Eletr, Z. M., and Wilkinson, K. D. (2011) An emerging model for BAP1's role in regulating cell cycle progression. *Cell Biochem. Biophys.* **60,** 3–11
8. Ismail, I. H., Davidson, R., Gagné, J. P., Xu, Z. Z., Poirier, G. G., and Hendzel, M. J. (2014) Germline mutations in BAP1 impair its function in DNA double-strand break repair. *Cancer Res.* **74,** 4282–4294
9. Yu, H., Pak, H., Hammond-Martel, I., Ghram, M., Rodrigue, A., Daou, S., Barbour, H., Corbeil, L., Hebert, J., Drobetsky, E., Masson, J. Y., Di Noia, J. M., and Affar, el. B. (2014) Tumor suppressor and deubiquitinase BAP1 promotes DNA double-strand break repair. *Proc. Natl. Acad. Sci. U.S.A.* **111,** 285–290
10. Dai, F., Lee, H., Zhang, Y., Zhuang, L., Yao, H., Xi, Y., Xiao, Z. D., You, M. J., Li, W., Su, X., and Gan, B. (2017) BAP1 inhibits the ER stress gene regulatory network and modulates metabolic stress response. *Proc. Natl. Acad. Sci. U.S.A.* **114,** 3192–3197
11. Ventii, K. H., Devi, N. S., Friedrich, K. L., Chernova, T. A., Tighiouart, M., Van Meir, E. G., and Wilkinson, K. D. (2008) BRCA1-associated protein-1 is a tumor suppressor that requires deubiquitinating activity and nuclear localization. *Cancer Res.* **68,** 6953–6962
12. Yu, M., Liang, H., Fu, Z., Wang, X., Liao, Z., Zhou, Y., Liu, Y., Wang, Y., Hong, Y., Zhou, X., Yan, X., Yu, M., Ma, M., Zhang, W., Guo, B., Zhang, J., Zen, K., Zhang, C. Y., Wang, T., Zhang, Q., and Chen, X. (2016) BAP1 suppresses lung cancer progression and is inhibited by miR-31. *Oncotarget* **7,** 13742–13753
13. Harbour, J. W., Onken, M. D., Roberson, E. D., Duan, S., Cao, L., Worley, L. A., Council, M. L., Matatall, K. A., Helms, C., and Bowcock, A. M. (2010) Frequent mutation of BAP1 in metastasizing uveal melanomas. *Science* **330,** 1410–1413
14. Bott, M., Brevet, M., Taylor, B. S., Shimizu, S., Ito, T., Wang, L., Creaney, J., Lake, R. A., Zakowski, M. F., Reva, B., Sander, C., Delsite, R., Powell, S., Zhou, Q., Shen, R., Olshen, A., Rusch, V., and Ladanyi, M. (2011) The nuclear deubiquitinase BAP1 is commonly inactivated by somatic mutations and 3p21.1 losses in malignant pleural mesothelioma. *Nat. Genet.* **43,** 668–672
15. Machida, Y. J., Machida, Y., Vashisht, A. A., Wohlschlegel, J. A., and Dutta, A. (2009) The deubiquitinating enzyme BAP1 regulates cell growth via interaction with HCF-1. *J. Biol. Chem.* **284,** 34179–34188
16. Misaghi, S., Ottosen, S., Izrael-Tomasevic, A., Arnott, D., Lamkanfi, M., Lee, J., Liu, J., O'Rourke, K., Dixit, V. M., and Wilson, A. C. (2009) Association of C-terminal ubiquitin hydrolase BRCA1-associated protein 1 with cell cycle regulator host cell factor 1. *Mol. Cell. Biol.* **29,** 2181–2192
17. Nishikawa, H., Wu, W., Koike, A., Kojima, R., Gomi, H., Fukuda, M., and Ohta, T. (2009) BRCA1-associated protein 1 interferes with BRCA1/BARD1 RING heterodimer activity. *Cancer Res.* **69,** 111–119
18. Arzt, L., Quehenberger, F., Halbwedl, I., Mairinger, T., and Popper, H. H. (2014) BAP1 protein is a progression factor in malignant pleural mesothelioma. *Pathol. Oncol. Res.* **20,** 145–151
19. Baumann, F., Flores, E., Napolitano, A., Kanodia, S., Taioli, E., Pass, H., Yang, H., and Carbone, M. (2015) Mesothelioma patients with germline BAP1 mutations have 7-fold improved long-term survival. *Carcinogenesis* **36,** 76–81
20. Shuch, B., Amin, A., Armstrong, A. J., Eble, J. N., Ficarra, V., Lopez-Beltran, A., Martignoni, G., Rini, B. I., and Kutikov, A. (2015) Understanding pathologic variants of renal cell carcinoma: Distilling therapeutic opportunities from biologic complexity. *Eur. Urol.* **67,** 85–97
21. Rini, B. I., Campbell, S. C., and Escudier, B. (2009) Renal cell carcinoma. *The Lancet* **373,** 1119–1132
22. Peña-Llopis, S., Vega-Rubín-de-Celis, S., Liao, A., Leng, N., Pavia-Jiménez, A., Wang, S., Yamasaki, T., Zhrebker, L., Sivanand, S., Spence,

P., Kinch, L., Hambuch, T., Jain, S., Lotan, Y., Margulis, V., Sagalowsky, A. I., Summerour, P. B., Kabbani, W., Wong, S. W., Grishin, N., Laurent, M., Xie, X. J., Haudenschild, C. D., Ross, M. T., Bentley, D. R., Kapur, P., and Brugarolas, J. (2012) BAP1 loss defines a new class of renal cell carcinoma. *Nat. Genet.* **44,** 751–759

23. Carlo, M. I., Manley, B., Patil, S., Woo, K. M., Coskey, D. T., Redzematovic, A., Arcila, M., Ladanyi, M., Lee, W., Chen, Y. B., Lee, C. H., Feldman, D. R., Hakimi, A. A., Motzer, R. J., Hsieh, J. J., and Voss, M. H. (2017) Genomic alterations and outcomes with VEGF-targeted therapy in patients with clear cell renal cell carcinoma. *Kidney Cancer* **1,** 49–56
24. Piva, F., Santoni, M., Matrana, M. R., Satti, S., Giulietti, M., Occhipinti, G., Massari, F., Cheng, L., Lopez-Beltran, A., Scarpelli, M., Principato, G., Cascinu, S., and Montironi, R. (2015) BAP1, PBRM1 and SETD2 in clear-cell renal cell carcinoma: Molecular diagnostics and possible targets for personalized therapies. *Expert Rev. Mol. Diagn.* **15,** 1201–1210
25. Gerlinger, M., Horswell, S., Larkin, J., Rowan, A. J., Salm, M. P., Varela, I., Fisher, R., McGranahan, N., Matthews, N., Santos, C. R., Martinez, P., Phillimore, B., Begum, S., Rabinowitz, A., Spencer-Dene, B., Gulati, S., Bates, P. A., Stamp, G., Pickering, L., Gore, M., Nicol, D. L., Hazell, S., Futreal, P. A., Stewart, A., and Swanton, C. (2014) Genomic architecture and evolution of clear cell renal cell carcinomas defined by multiregion sequencing. *Nat. Genet.* **46,** 225–233
26. Oosterwijk, E., Rathmell, W. K., Junker, K., Brannon, A. R., Pouliot, F., Finley, D. S., Mulders, P. F., Kirkali, Z., Uemura, H., and Belldegrun, A. (2011) Basic research in kidney cancer. *Eur. Urol.* **60,** 622–633
27. Ran, F. A., Hsu, P. D., Wright, J., Agarwala, V., Scott, D. A., and Zhang, F. (2013) Genome engineering using the CRISPR-Cas9 system. *Nat. Protoc.* **8,** 2281–2308
28. Zhou, J., Wang, J., Shen, B., Chen, L., Su, Y., Yang, J., Zhang, W., Tian, X., and Huang, X. (2014) Dual sgRNAs facilitate CRISPR/Cas9-mediated mouse genome targeting. *FEBS J.* **281,** 1717–1725
29. Lee, A. (2012) RhoGTPase Activation assay. *Bio-Protocol* **2,** e269
30. Kim, T. H., and Dekker, J. (2018) ChIP. *Cold Spring Harb. Protoc.* **2018,** pdb prot082610
31. Anaya, J. (2016) OncoLnc: Linking TCGA survival data to mRNAs, miRNAs, and lncRNAs. *Peerj. Comput. Sci.* **2,** e67
32. Cancer Genome Atlas Research Network (2013) Comprehensive molecular characterization of clear cell renal cell carcinoma. *Nature* **499,** 43–49
33. Gan, C. S., Chong, P. K., Pham, T. K., and Wright, P. C. (2007) Technical, experimental, and biological variations in isobaric tags for relative and absolute quantitation (iTRAQ). *J. Proteome Res.* **6,** 821–827
34. Thiery, J. P., Acloque, H., Huang, R. Y., and Nieto, M. A. (2009) Epithelial-mesenchymal transitions in development and disease. *Cell* **139,** 871–890
35. Ye, X., and Weinberg, R. A. (2015) Epithelial-mesenchymal plasticity: A central regulator of cancer progression. *Trends Cell Biol.* **25,** 675–686
36. Hanahan, D., and Weinberg, R. A. (2000) The hallmarks of cancer. *Cell* **100,** 57–70
37. Hanahan, D., and Weinberg, R. A. (2011) Hallmarks of cancer: The next generation. *Cell* **144,** 646–674
38. Cano, A., Perez-Moreno, M. A., Rodrigo, I., Locascio, A., Blanco, M. J., del Barrio, M. G., Portillo, F., and Nieto, M. A. (2000) The transcription factor Snail controls epithelial-mesenchymal transitions by repressing E-cadherin expression. *Nature Cell Biol.* **2,** 76–83
39. Zhou, W., Zhu, P., Wang, J., Pascual, G., Ohgi, K. A., Lozach, J., Glass, C. K., and Rosenfeld, M. G. (2008) Histone H2A monoubiquitination represses transcription by inhibiting RNA polymerase II transcriptional elongation. *Mol. Cell* **29,** 69–80
40. Kalb, R., Latwiel, S., Baymaz, H. I., Jansen, P. W., Müller, C. W., Vermeulen, M., and Müller, J. (2014) Histone H2A monoubiquitination promotes histone H3 methylation in Polycomb repression. *Nat. Struct. Mol. Biol.* **21,** 569–571
41. Kaibuchi, K., Kuroda, S., and Amano, M. (1999) Regulation of the cytoskeleton and cell adhesion by the Rho family GTPases in mammalian cells. *Annu. Rev. Biochem.* **68,** 459–486
42. Raftopoulou, M., and Hall, A. (2004) Cell migration: Rho GTPases lead the way. *Dev. Biol.* **265,** 23–32
43. Henderson, V., Smith, B., Burton, L. J., Randle, D., Morris, M., and Odero-Marah, V. A. (2015) Snail promotes cell migration through PI3K/AKT-dependent Rac1 activation as well as PI3K/AKT-independent pathways during prostate cancer progression. *Cell Adhes. Migr.* **9,** 255–264
44. Shields, M. A., Krantz, S. B., Bentrem, D. J., Dangi-Garimella, S., and Munshi, H. G. (2012) Interplay between beta1-integrin and Rho signaling regulates differential scattering and motility of pancreatic cancer cells by snail and Slug proteins. *J. Biol. Chem.* **287,** 6218–6229
45. Belgiovine, C., Chiesa, G., Chiodi, I., Frapolli, R., Bonezzi, K., Taraboletti, G., D'Incalci, M., and Mondello, C. (2016) Snail levels control the migration mechanism of mesenchymal tumor cells. *Oncol. Lett.* **12,** 767–771
46. Zhang, A., Wang, Q., Han, Z., Hu, W., Xi, L., Gao, Q., Wang, S., Zhou, J., Xu, G., Meng, L., Chen, G., and Ma, D. (2013) Reduced expression of Snail decreases breast cancer cell motility by downregulating the expression and inhibiting the activity of RhoA GTPase. *Oncol. Lett.* **6,** 339–346
47. de Cubas, A. A., and Rathmell, W. K. (2018) Epigenetic modifiers: Activities in renal cell carcinoma. *Nat. Rev. Urol.* **15,** 599–614
48. Sanchez, D. J., and Simon, M. C. (2018) Genetic and metabolic hallmarks of clear cell renal cell carcinoma. *Biochim. Biophys. Acta* **1870,** 23–31
49. Fahey, C. C., and Davis, I. J. (2017) SETting the stage for cancer development: SETD2 and the consequences of lost methylation. *Cold Spring Harb .Perspect. Med.* **7,** a026468
50. Yu, H., Mashtalir, N., Daou, S., Hammond-Martel, I., Ross, J., Sui, G., Hart, G. W., Rauscher, F. J., 3rd, Drobetsky, E., Milot, E., Shi, Y., and Affar el, B. (2010) The ubiquitin carboxyl hydrolase BAP1 forms a ternary complex with YY1 and HCF-1 and is a critical regulator of gene expression. *Mol. Cell. Biol.* 30, 5071–5085
51. Brunot, A., Bernhard, J. C., Yacoub, M., Edeline, J., Verhoest, G., Bensalah, K., Dupuis, F., Laguerre, B., Kerbrat, P., Ravaud, A., Bellaud, P., Viel, R., Jouan, F., Rioux-Leclercq, N., and Kammerer-Jacquet, S. F. (2015) PDL-1 and PDL1 expressions in clear cell renal cell carcinoma (ccRCC) of metastatic patients with sunitinib first-line treatment. *J. Clin. Oncol.* **33,** e14002
52. Kammerer-Jacquet, S. F., Crouzet, L., Brunot, A., Dagher, J., Pladys, A., Edeline, J., Laguerre, B., Peyronnet, B., Mathieu, R., Verhoest, G., Patard, J. J., Lespagnol, A., Mosser, J., Denis, M., Messai, Y., Gad-Lapiteau, S., Chouaib, S., Belaud-Rotureau, M. A., Bensalah, K., and Rioux-Leclercq, N. (2017) Independent association of PD-L1 expression with noninactivated VHL clear cell renal cell carcinoma-A finding with therapeutic potential. *Int. J. Cancer* **140,** 142–148
53. Chen, L., Gibbons, D. L., Goswami, S., Cortez, M. A., Ahn, Y. H., Byers, L. A., Zhang, X., Yi, X., Dwyer, D., Lin, W., Diao, L., Wang, J., Roybal, J., Patel, M., Ungewiss, C., Peng, D., Antonia, S., Mediavilla-Varela, M., Robertson, G., Jones, S., Suraokar, M., Welsh, J. W., Erez, B., Wistuba, I. I., Chen, L., Peng, D., Wang, S., Ullrich, S. E., Heymach, J. V., Kurie, J. M., and Qin, F. X. (2014) Metastasis is regulated via microRNA-200/ZEB1 axis control of tumour cell PD-L1 expression and intratumoral immunosuppression. *Nat. Commun.* **5,** 5241